

Investigation of real-time and complementary particle discrimination capabilities in FAUST

T. Hankins, A. Hannaman, A.B. McIntosh, K. Hagel, B. Harvey, Z. Tobin, and S.J. Yennello

CsI(Tl) scintillating crystals as particle detectors exhibit a particle dependent light response; the optical characteristics of the light response, including absolute light output, rise time, and various decay times, provide multiple methods by which incident particles can be identified [1]. These particle identification (PID) methods have been shown to display varying degrees of success, ranging from standard Z discrimination [2] to stellar isotopic resolution [3]. In the case of the Forward Array Using Silicon Technology (FAUST), utilization of the zero-crossing time (ZCT) versus amplitude discrimination scheme resulted in defined isotopic resolution of hydrogen and clear discretization between ${}^8\text{Li}$ and α - α double hits [4].

Despite this success, problems can be encountered when employing alternate discrimination methods for data obtained from an array configuration involving secondary or tertiary detectors. In the case of FAUST, a demand for increased position sensitivity and angular resolution lead to the inclusion of a tertiary Duo-Axis Dual-Lateral (DADL) silicon detector layer. In this configuration, event triggering occurs based on signals received from the DADL and the CsI(Tl) crystal. This gives rise to a key issue: as a result of their low ionization density and stopping power, high energy protons can be improperly detected by failing to trigger the DADL but still triggering the crystal. In this instance, particle discrimination methods relying on DADL energies suffer. This problem has founded a desire for an alternate PID method that can work in tandem with a primary method (such as ZCT vs. Amplitude) and “recover” lost information. One method that does not rely on a secondary detector is pulse-shape discrimination, which instead relies directly on the characteristics of the CsI(Tl) scintillation response and therefore does not suffer as a result of missing secondary input. It is important to note that pulse-shape discrimination methods are normally not used independently or in place of other identification methods because most alternates outperform it [2], but nonetheless can provide rudimentary PID without relying on external information. As a result, the first focus of this work involves investigating the viability of pulse-shape discrimination as a supplement to particle identification methods dependent on external triggering.

Another potential issue encountered involves the event readout chain. Depending on the particle identification method, integration of either the raw or smoothed CsI(Tl) waveform is used [5]. Performing this method requires the waveform for every event be written to disk; in addition to commandeering large amounts of disk space, this approach severely inhibits the rate at which events can be read out (event rate saturation). However, the Struck Innovative Systems (SIS) 3316 VME waveform digitizer that is part of the electronics chain possesses eight integrators that perform real-time integrations of raw waveforms. Traditionally, one integrator is used to calculate the baseline of the waveform and, often, the second is used to calculate the maximum of the waveform, leaving six that can be distributed at times relative to the internal trigger. Studying the behavior of the waveforms produced by the CsI(Tl) crystal may provide insight regarding the plausibility of real-time particle discrimination using the remaining six integrators, rather than reading out entire waveforms and performing PID offline; this is the second focus of this work.

Data used in the subsequent analyses were obtained using 20 MeV/u ^{20}Ne incident on 3.1 mg/cm^2 ^{12}C ; acquisition was conducted using a singular CsI(Tl) crystal optically coupled to a lucite light guide and a PIN photodiode and a DADL detector. Signals from the DADL and the CsI(Tl) crystal were read into SIS3316 digitizers programmed with a $0.75\text{ }\mu\text{s}$ pre-trigger delay.

Various PSD-related methodologies have been explored in this research. In the event that waveform characteristics were desired or waveforms had a low signal to noise ratio (SNR), information was retrieved via fit. The method used herein was of exponential functional form and minimized using the Minuit package built into the data analysis framework ROOT. The method was further improved through χ^2 and parameter variance guided trial-and-error optimization that permitted accurate fitting of waveforms independent of intrinsic SNR (Fig. 1). The most successful and therefore most explored approach was that of charge comparison, in which the waveform for each event is integrated in two separate regions, often denoted “slow” and “fast” (in reference to the nature of the decay components of CsI(Tl) scintillations), and then plotted against each other (Fig. 2). Efficiency of the method is determined based primarily on the degree of band separation, quantitated using figure-of-merit (FOM), and secondarily by the degree of spillover. Figure-of-merit is defined as the separation between the centroids of the peaks in a plot divided by the sum of the peak full widths at half maximum (FWHM) [5]; spillover is the measurement of the

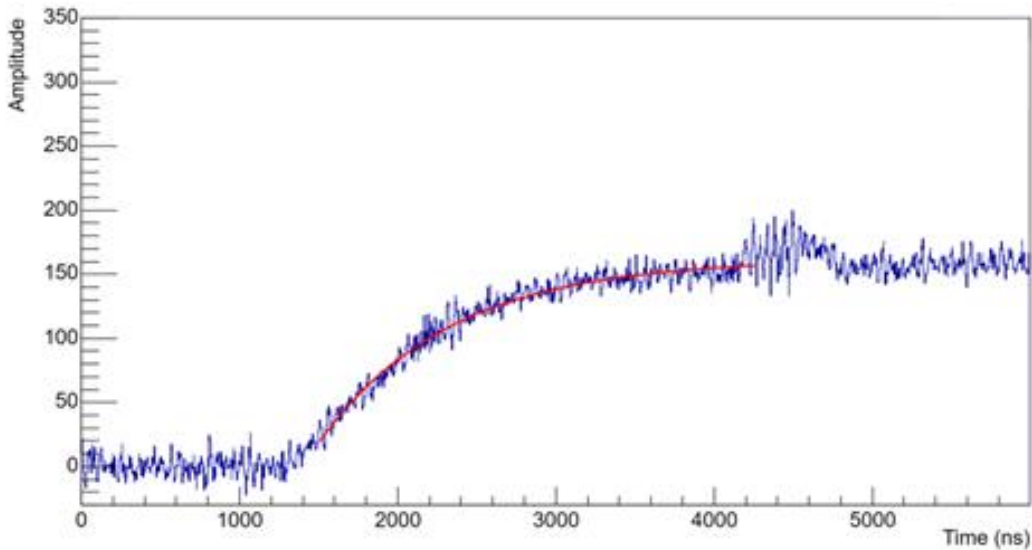


Fig. 1. Characteristic CsI(Tl) waveform (blue) superimposed with fit (red). The fit was produced using method described in the text; fit parameters have been omitted from the figure for simplicity.

percentage of events of a particular type of radiation misclassified as another type by localization in an incorrect region of interest (ROI) [2]. Spillover percentages for protons (p) and α particles are calculated

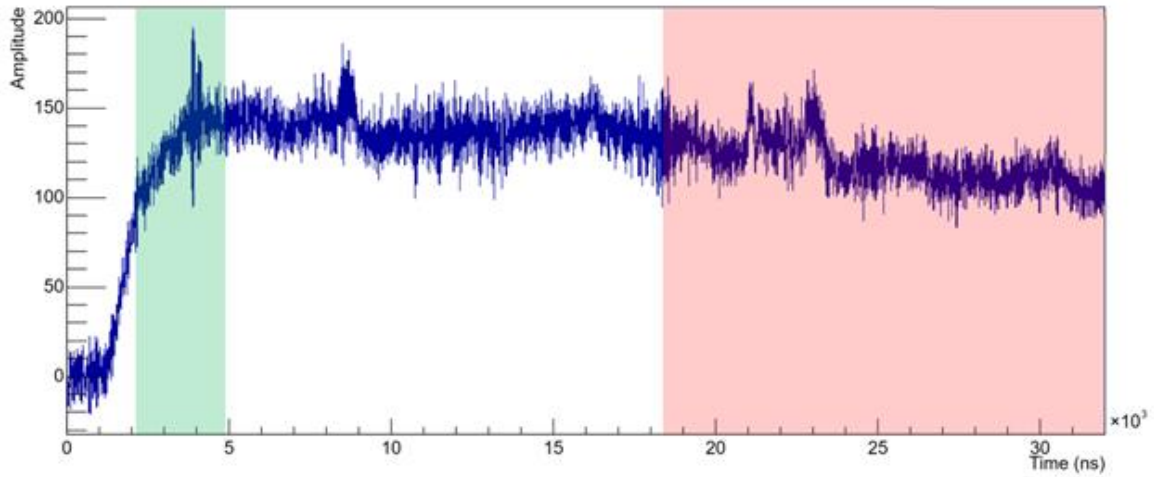


Fig. 2. Characteristic CsI(Tl) waveform (blue) superimposed with integration windows for the slow (red) and fast (green) components that yielded the greatest FOM.

by gating on localized bands in a $\Delta E-E$ plot, producing respective slow-fast plots, and determining the associated degrees of mismatch. Figures-of-merit are calculated by dividing the values in slow-fast space by either the slow or fast integration value, thus producing a resultant plot of arbitrary PID index versus the slow or fast value. This plot is then horizontally projected to produce a one-dimensional plot dependent solely on the PID index. The peaks present are fit with Gaussian functions and the associated FOM is determined from the parameters of the fits.

At the time of writing, the largest FOM achieved has been 0.981 (Fig. 2), accomplished using a slow integration across the last 13.6 μs of the total 32.0 μs waveform and a fast integration of 2.8 μs

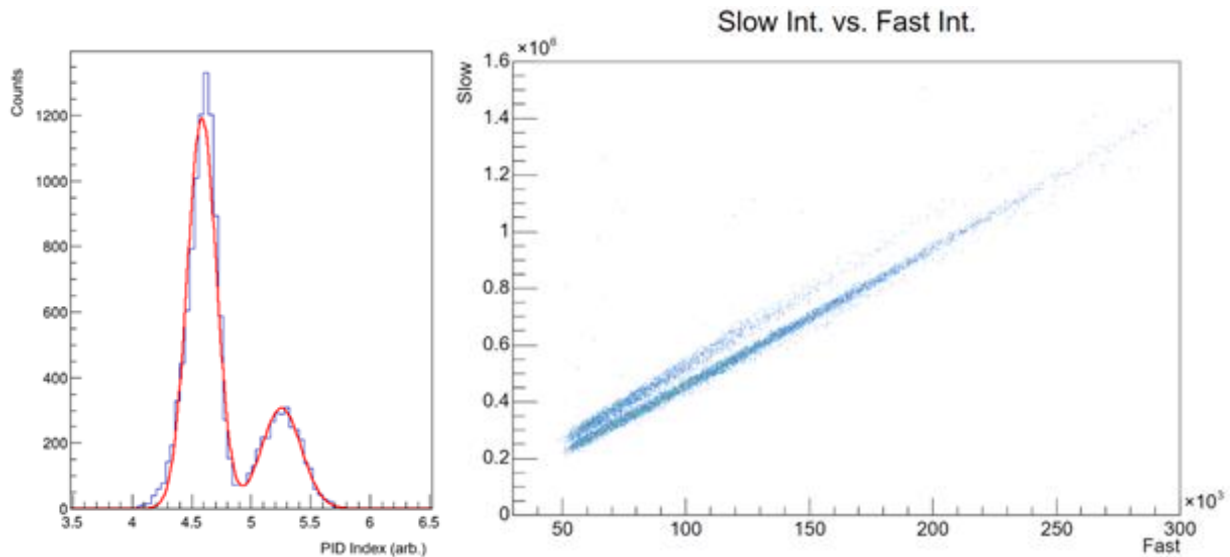


Fig. 3. Left: horizontal projection of the PID index versus number of events (counts). The FOM for this projection is 0.981; p are identified by the right peak and α by the left peak. Right: corresponding slow-fast plot of experimental data. Z-discrimination is achieved by clear band separation; isotopic resolution remains unfulfilled.

starting at an absolute time of 2.04 μ s. Additionally, this configuration possessed spillover percentages of 8.94 and 1.81 for p into α and α into p , respectively. This optimization comes as a surprise; this fast configuration misses a substantial amount of the rise component of the CsI waveform (Fig. 3) which is what exhibits the greatest dependence on incident particle type [5]. Further investigation as to why this occurs is currently underway, but the Z discrimination achieved through pulse-shape integration of the waveform through predefined windows suggests that it may be possible to perform some degree of real-time particle discrimination using integrators. A FOM of 0.937 and maximum spillover of 8.94% bode well for online proton and alpha discrimination, but isotopic resolution has as of yet remained unfulfilled.

- [1] R. S. Storey, W. Sack, and A. Ward, Proc. Phys. Soc. (London) **72**, 1 (1958).
- [2] P. Chandrikamohan and T. DeVol, IEEE Trans. on Nucl. Sci. **54**, 2 (2007)
- [3] M. Alderighi *et al.*, Nucl. Instrum. Methods Phys. Res. **A489**, 257 (2002).
- [4] R. Laforest *et al.*, Nucl. Instrum. Methods Phys. Res. **A404**, 470 (1998).
- [5] W. Skulski and M. Momayezi, Nucl. Instrum. Methods Phys. Res. **A458**, 759 (2001).